BJPS

Brazilian Journal of
Pharmaceutical Sciences

http://dx.doi.org/10.1590/s2175-97902023e22476

Article

Swertiamarin attenuates paraquat-induced pulmonary epithelial-like cell apoptosis via NOX4-mediated regulation of redox and mitochondrial function

Ji Wu[1,†], Yong Li[2,†], Xinju Li[3], Tao Wu[2,*]

[1]Department of Medicine, Wuhan City College, Wuhan, China, [2]Department of Pharmacy, Wuhan Fourth Hospital, Wuhan, China, [3]Department of Blood Transfusion, Weifang People's Hospital, Weifang, China

[†]This author contributed equally to this work.

The aim of the present study was to investigate the effect of swertiamarin (STM) in attenuating paraquat (PQ)-induced human lung alveolar epithelial-like cell (A549) apoptosis and the underlying mechanisms. A549 cells were pretreated with different concentrations of STM for 2 hr and then cultured with or without PQ (700 μM) for 24 hr. Cell survival was determined using the CCK8 assay. Morphological changes, MDA content, inflammatory factors, fibrogenesis parameters, apoptosis rates, redox status and mitochondrial membrane potential (MMP) were evaluated. The expression of several genes involved in the modulation of redox status was measured by Western blotting. Cell viability and MMP were decreased, but the apoptosis rate and DCFH oxidation were elevated by PQ exposure. STM pretreatment notably increased cell viability and MMP and reduced the apoptosis rate and DCFH oxidation. Furthermore, TLR4-NOX4 signaling was significantly inhibited by STM. The downregulation of NOX4 by siRNA exerted the same protective effects as STM. This study provides the first evidence that STM attenuates PQ-induced pulmonary epithelial-like cell apoptosis via NOX4-mediated regulation of redox and mitochondrial function.

Keywords: Swertiamarin. Alveolar epithelial cells. Paraquat. siRNA. NOX4

INTRODUCTION

Paraquat (PQ) is a widely used and highly toxic herbicide in many countries, especially in developing countries. PQ poisoning results in multiple organ failure in animals and humans, and the lung is the principle target organ of PQ poisoning (Novaes *et al*., 2016). This is because PQ is more concentrated in lung tissue than in any other organ. PQ accumulates in the lung through type II airway epithelial cells (AECIIs) via a polyamine uptake system. After PQ enters the lungs, it produces a large amount of oxygen free radicals and various inflammatory factors, leading to the rapid proliferation of various inflammatory cells, acute lung injury, and finally pulmonary fibrosis and respiratory failure (Wynn, 2007). Pulmonary toxicity is the most common complication in the treatment of PQ poisoning (Gawarammana, Buckley, 2011). Despite the high mortality rate of PQ-induced pulmonary fibrosis, the mechanism by which PQ induces pulmonary fibrosis is still not fully understood.

Strategies for attenuating the toxicity of PQ have been proposed, including the induction of vomiting, hemoperfusion, scavenging oxygen free radicals and the prevention of pulmonary fibrosis (Blanco-Ayala, Andérica-Romero, Pedraza-Chaverri, 2014). However, those treatments still have no confirmed effects on improving survival (Loveman *et al*., 2014). Thus, extensive studies on effective antifibrotic medicines are urgently needed. Recently, some synthetic or natural

***Correspondence:** Tao Wu. Department of Pharmacy. Wuhan Fourth Hospital. No. 473 Hanzheng Street. Qiaokou District, Wuhan, Hubei Province, 430033, China. Phone: +8602768831991. E-mail: hydrinsk@sina.com. ORCID: https://orcid.org/0000-0003-3638-5283

molecules have exerted protective effects against PQ-induced experimental pulmonary fibrosis in the laboratory. For instance, cyclosporine can inhibit PQ-induced mitophagy and pulmonary fibrosis by attenuating PINK1/Parkin signaling (Liu *et al*., 2020). Arctigenin suppresses PQ-induced pulmonary fibrosis through the Wnt3a/β-Catenin pathway *in vivo* and *in vitro* (Gao *et al*., 2020).

Swertiamarin (STM) is a bitter secoiridoid glycoside isolated from *Swertia mussotii* Franch (Gentianaceae) that exerts hepatoprotective and anti-inflammatory effects (Zhang *et al*., 2019; Saravanan *et al*., 2014). Many cases of experimental organ fibrosis have been improved by STM, and STM has opened a new promising window for the prognosis of fibrotic diseases (Li *et al*., 2016; Chen *et al*., 2019). We previously demonstrated that STM could protect against carbon tetrachloride-induced hepatic fibrosis in rats by alleviating oxidative stress and inhibiting TLR4 signals (Wu *et al*., 2017; Wu, Zhang, Song, 2018). In the present study, we hypothesize that STM attenuates pulmonary fibrosis by modulating redox status and fibrogenesis. To test this hypothesis, we investigated the effect of STM on PQ-induced injury in human lung alveolar epithelial-like cells (A549).

MATERIAL AND METHODS

Chemicals and antibodies

Swertiamarin (SC-474478) was provided by Santa Cruz Biotechnology, Inc. Paraquat was provided by Sigma–Aldrich (St. Louis, MO, USA). Primary antibodies against TLR4 (PAB33926) and NOX4 (PAB30655) were purchased from Bioswamp (Wuhan, China). Antibodies against β-actin (no. 4967) were provided by Cell Signaling Technology (Danvers, MA, USA). F12K medium and fetal bovine serum (FBS) were provided by Gibco (Rockville, MD, USA). All other chemicals and reagents used in this study were of analytical grade.

In vitro assays

siRNA transfection

According to the full-length cDNA sequence of NOX4 in GenBank, a specific sequence was selected as the target of interference (interference sequence: GGACCCAATTCACTATCCA). The NOX4-siRNA oligo and control siRNA oligonucleotides were synthesized by RIBOBIO, Inc. (Guangzhou, China). Human alveolar type II-like epithelial A549 cells were seeded in a 6-well plate at a density of 5×10^5 cells/well. When the cells were grown to 90% confluence, NOX4-siRNA (50 nmol/L) or negative control (NC) was transfected into the cells with Lipofectamine® RNAiMAX according to the manufacturer's instructions. After 24 h, the supernatant was replaced with fresh medium.

Cell culture

Human alveolar type II-like epithelial A549 cells were purchased from the Cell Bank of the Chinese Academy of Sciences (Shanghai, China). A549 cells were cultured in F12K medium supplemented with 10% heat inactivated FBS and antibiotics (100 IU/mL penicillin and 100 μg/mL streptomycin) at 37 °C with 5% CO_2 in a humidified incubator, and the cells were subcultured until they were 80–90% confluent. PQ was dissolved in distilled water to make stock solutions, and DMSO was used as the solvent for swertiamarin. Before the experiment, A549 cells were pretreated for 2 hr with different concentrations of swertiamarin (50, 100, 200 μM).

Morphological Changes

To study the effect of swertiamarin (STM) on morphological changes, A549 cells were seeded at a density of 10×10^4 cells/well in 12-well plates, and STM treatment was conducted before PQ (700 μM) treatment. Images were taken at 24 hr, and alterations in cellular morphology were observed under a microscope (×100, Nikon inverted microscope).

Cytotoxicity assay

The viability of A549 cells was detected with the Cell Counting Kit-8 (CCK-8) assay (Beyotime Biotechnology, China). A549 cells (5×10^3/well) were seeded into 96-well Plates 24 hr prior to STM (50, 100, 200 μM) treatment. After 24 h of PQ treatment, the same volume of CCK-8 solution was added, and the cells were incubated for 1 hr at 37 °C. The absorption value of each well was measured with a multimode reader. Independent assays were performed three times in triplicate. The absorbance was evaluated at 450 nm using a spectrophotometer (BioTek, Winooski, VT, USA).

Measurement of oxidative stress, inflammation and fibrogenesis parameters

The levels of malondialdehyde (MDA), inflammatory cytokines (TNF-α and IL-8) and fibrogenesis parameters (Col-I and hydroxyproline) in the cell culture medium were assessed using ELISA kits. Briefly, the cells were cultured in 24-well plates (2×10^5 cells per well), and after the indicated treatments, the culture supernatants were collected, and the concentrations of MDA, TNF-α, IL-8, Col-I and hydroxyproline were measured by using the following commercial kits according to the manufacturer's instructions: Human malondialdehyde (MDA) ELISA Kit (HM10250, Bioswamp, China), Human Tumor necrosis factor α (TNF-α) ELISA Kit (HM10001, Bioswamp, China), Human Interleukin 8 (IL-8) ELISA Kit (HM10222, Bioswamp, China), Human Collagen Type I (Col -I) ELISA Kit (HM10125, Bioswamp, China), and Human hydroxyproline (Hyp) ELISA Kit (HM11025, Bioswamp, China).

Apoptosis assay

The apoptotic rate was detected by performing an Annexin V-FITC/PI staining assay using an Annexin V-FITC/PI Apoptosis Detection Kit (BD Biosciences, USA). Briefly, at the end of the treatment, A549 cells were collected and incubated with the working solution (Annexin V-FITC (10 μL) and PI (10 μL)) at 4 °C for 0.5 hr in the dark. After being washed with PBS, the cells were detected by flow cytometry (ACEA NovoCyte, USA) according to the instructions.

Redox status assessment

Redox status assessment was conducted by using the probes dichlorofluorescein diacetate (DCFH-DA, Sigma, St. Louis, MO). Briefly, after the end of the treatment, the cells were digested and suspended. After centrifugation, the cells were incubated with DCFH-DA (10 μM) at 37 °C for 0.5 hr in the dark, washed with PBS, resuspended and examined by flow cytometry (ACEA NovoCyte, USA). The data were collected and analyzed using NovoCyte software.

Mitochondrial membrane potential (MMP) measurement

To determine MMP, the cells were stained with a JC-1 Mitochondrial Membrane Potential Assay Kit (Bioswamp) according to the manufacturer's instructions and subsequently analyzed by flow cytometry with CXP software 2.0.

Immunoblotting analysis (TLR4-NOX4 signaling)

A549 cell lysates were prepared with RIPA buffer containing a protease inhibitor cocktail, and the protein concentration was determined using a BCA kit. Equal amounts of protein were separated on 12% SDS–PAGE gels and then transferred to nitrocellulose membranes. The membranes were blocked with blocking buffer (5% BSA in Tris-buffered saline with 0.01% T-Tween 20) for 2 h, followed by incubation with primary antibodies against TLR4 (1:1000, Bioswamp), NOX4 (1:1000, Bioswamp) and β-actin (1:1000, CST) overnight at 4 °C. After the membranes were washed with TBST for 15 min, the membranes were incubated with HRP-conjugated secondary antibodies for 1 h at room temperature and subsequently processed for ECL detection using a potent ECL kit (Millipore, USA) and a chemiluminescence detection system (IS4000MM Pro, Kodak, USA). Actin was used as an internal control, and the densitometric values of the bands were determined and statistically analyzed using ImageJ software.

Data analysis

The data are expressed as the mean ± S.D. Significant differences between groups were assessed with SPSS version 13.0. Comparisons of results were performed by one-way analysis of variance followed by Tukey's post hoc test for multiple comparisons. Differences were considered statistically significant when $p < 0.05$ and extremely significant when $p < 0.01$.

RESULTS AND DISCUSSION

Effect of STM on PQ-induced cytotoxicity and morphological changes

The viability of A549 cells following treatment with PQ (700 μM) or vehicle for 24 h was examined with CCK8 assays. As shown in Figure 1, A549 cell survival rates were markedly inhibited by PQ in comparison with the control group. STM dose-dependently attenuated PQ-induced cytotoxicity in A549 cells. The morphological changes in A549 cells were also improved by STM.

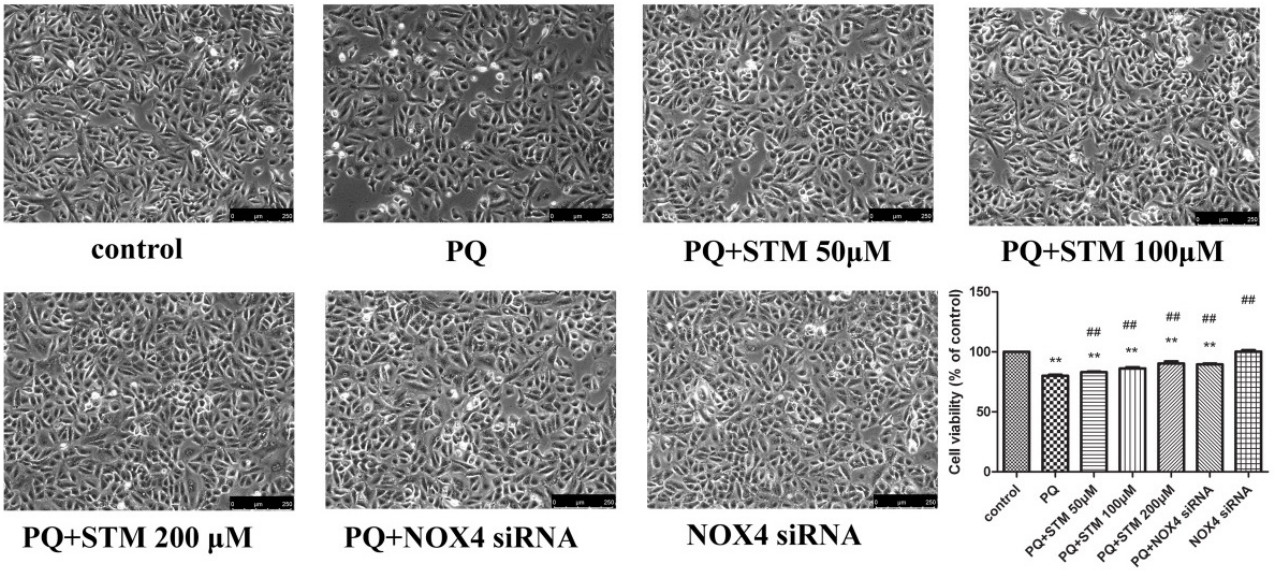

FIGURE 1 - STM protects A549 cells against PQ-induced cytotoxicity. CCK-8 assays revealed that STM alleviated PQ-induced cytotoxicity in A549 cells. STM improved PQ-induced morphological changes in A549 cells. NOX4 silencing ameliorated PQ-induced cytotoxicity in A549 cells. The data were obtained from six independent experiments. The results are represented as the means ± S.D.s. $^{**}p<0.01$ versus control; $^{\#\#}p<0.01$ versus PQ, determined using one-way ANOVA with Tukey's post hoc analysis.

Effect of STM on PQ-induced levels of MDA, inflammatory factors and fibrogenesis parameters

PQ (700 μM) stimulated the generation of MDA, TNF-α, IL-8, hydroxyproline and Col-I in A549 cells and enhanced the release of these cytokines into the culture medium (Figure 2A-E). STM dose-dependently attenuated PQ-induced cytokine production in A549 cells. Thus, STM could protect A549 cells from PQ-induced pulmonary fibrogenesis and inflammatory responses.

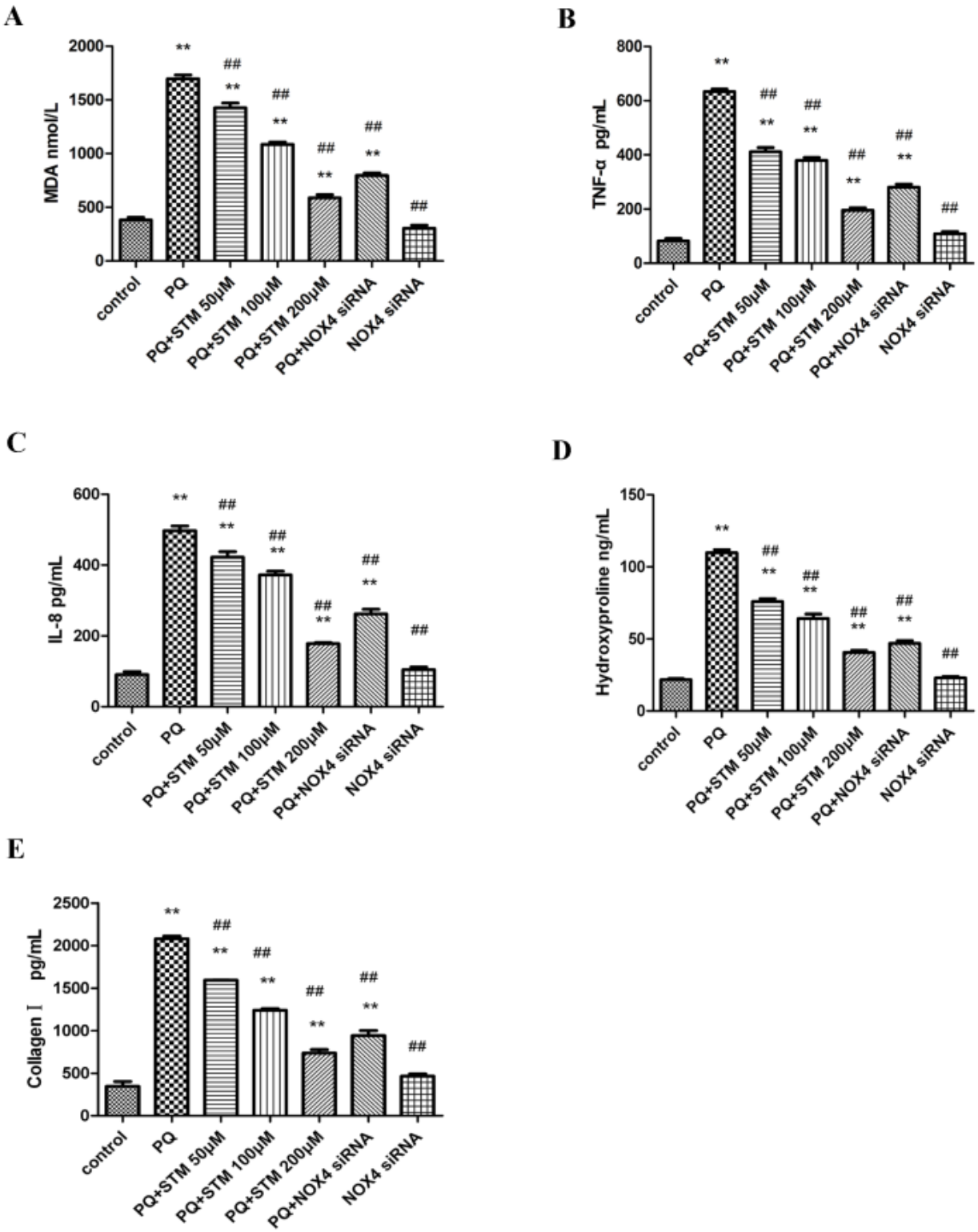

FIGURE 2 - STM reduced PQ-induced levels of MDA, inflammatory factors and fibrogenesis parameters in A549 cells. A: MDA; B: TNF-α; C: IL-8; D: Hydroxyproline; E: Collagen I. PQ increased the levels of MDA, inflammatory factors and fibrogenesis parameters of A549 cells. Pretreatment with STM (50, 100 and 200 μM) or NOX4 silencing resulted in decreases in the levels of MDA, inflammatory factors and fibrogenesis parameters. The data were obtained from at least three independent experiments. The results are represented as the means ± S.D.s. $^{**}p<0.01$ versus control; $^{\#\#}p<0.01$ versus PQ, determined using one-way ANOVA with Tukey's post hoc analysis.

STM alleviated PQ-induced A549 cell apoptosis and mitochondrial damage

To further characterize PQ-induced mitochondrial damage, a JC-1 assay was conducted to determine the ΔΨm of A549 cells by flow cytometry. PQ reduced the ΔΨm of A549 cells, and pretreatment with STM resulted in marked increases in ΔΨm (Figure 3).

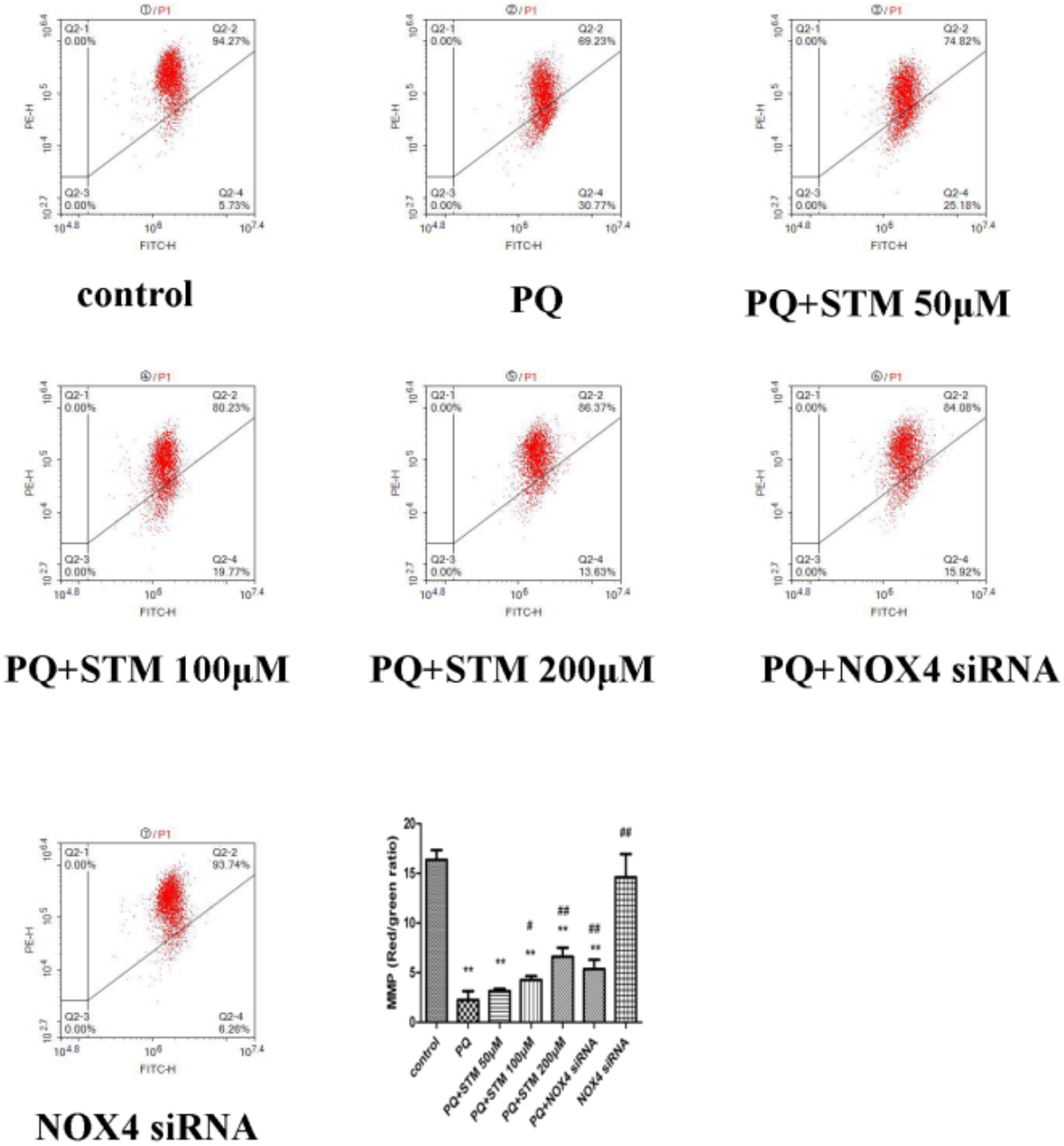

FIGURE 3 - Attenuation of PQ-induced mitochondrial dysfunction by STM. PQ exposure reduced the ΔΨm of A549 cells, and pretreatment with STM (50, 100 and 200 μM) or NOX4 silencing resulted in an increase in ΔΨm. The data were obtained from at least three independent experiments. The results are represented as the means ± S.D.s. $^{**}p<0.01$ versus control; $^{\#}p<0.05$ versus PQ, $^{\#\#}p<0.01$ versus PQ, determined using one-way ANOVA with Tukey's post hoc analysis.

To confirm PQ-induced apoptosis, A549 cells were double-stained with Annexin V and PI. Then, flow cytometry was performed to detect apoptotic cells. As shown in Figure 4, the apoptosis rate was markedly increased by PQ in A549 cells. Pretreatment with STM significantly reduced the apoptotic rate compared with PQ alone.

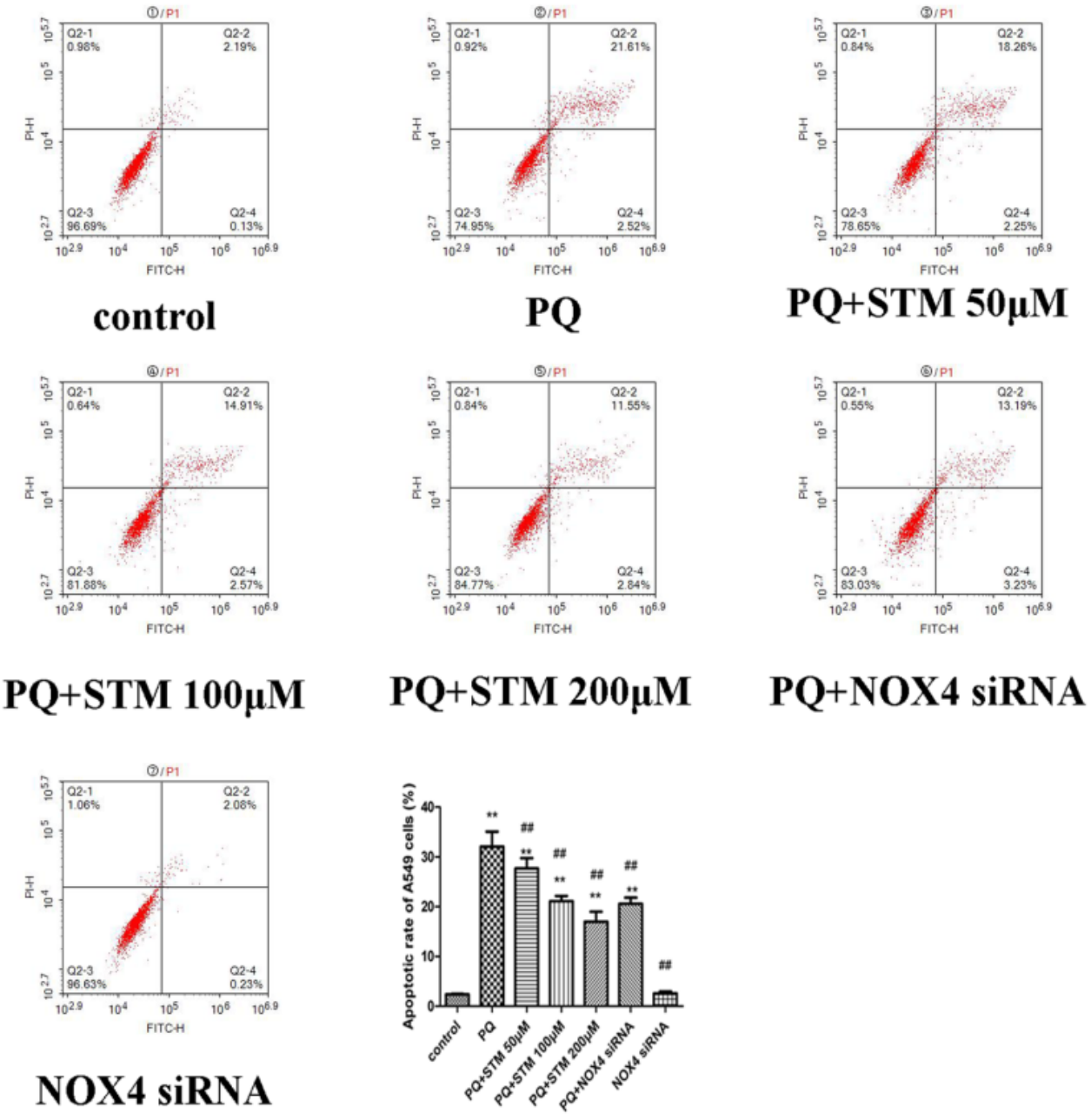

FIGURE 4 - Attenuation of PQ-induced apoptosis by STM. The proportion of apoptotic cells was measured using an Annexin V-FITC/PI assay. The apoptotic rate was significantly higher in the PQ group than in the control group ($p < 0.01$). Pretreatment with STM (50, 100 and 200 μM) or NOX4 silencing significantly decreased the apoptotic rate compared with PQ treatment alone ($p < 0.05$ or 0.01). The data were obtained from at least three independent experiments. The results are represented as the means ± S.D.s. $^{**}p<0.01$ versus control; $^{\#}p<0.05$ versus PQ, $^{\#\#}p<0.01$ versus PQ, determined using one-way ANOVA with Tukey's post hoc analysis.

STM pretreatment ameliorated PQ-induced redox imbalance

To explore whether STM has antioxidant effects, redox status was evaluated after PQ exposure. As shown in Figure 5, DCF fluorescence intensity was measured by flow cytometry and indicated that PQ exposure enhanced intracellular iron signaling or peroxynitrite formation. In contrast, STM (100 and 200 μM) pretreatment or NOX4 siRNA significantly reduced DCF fluorescence intensity, thus ameliorating PQ-induced redox imbalance in A549 cells.

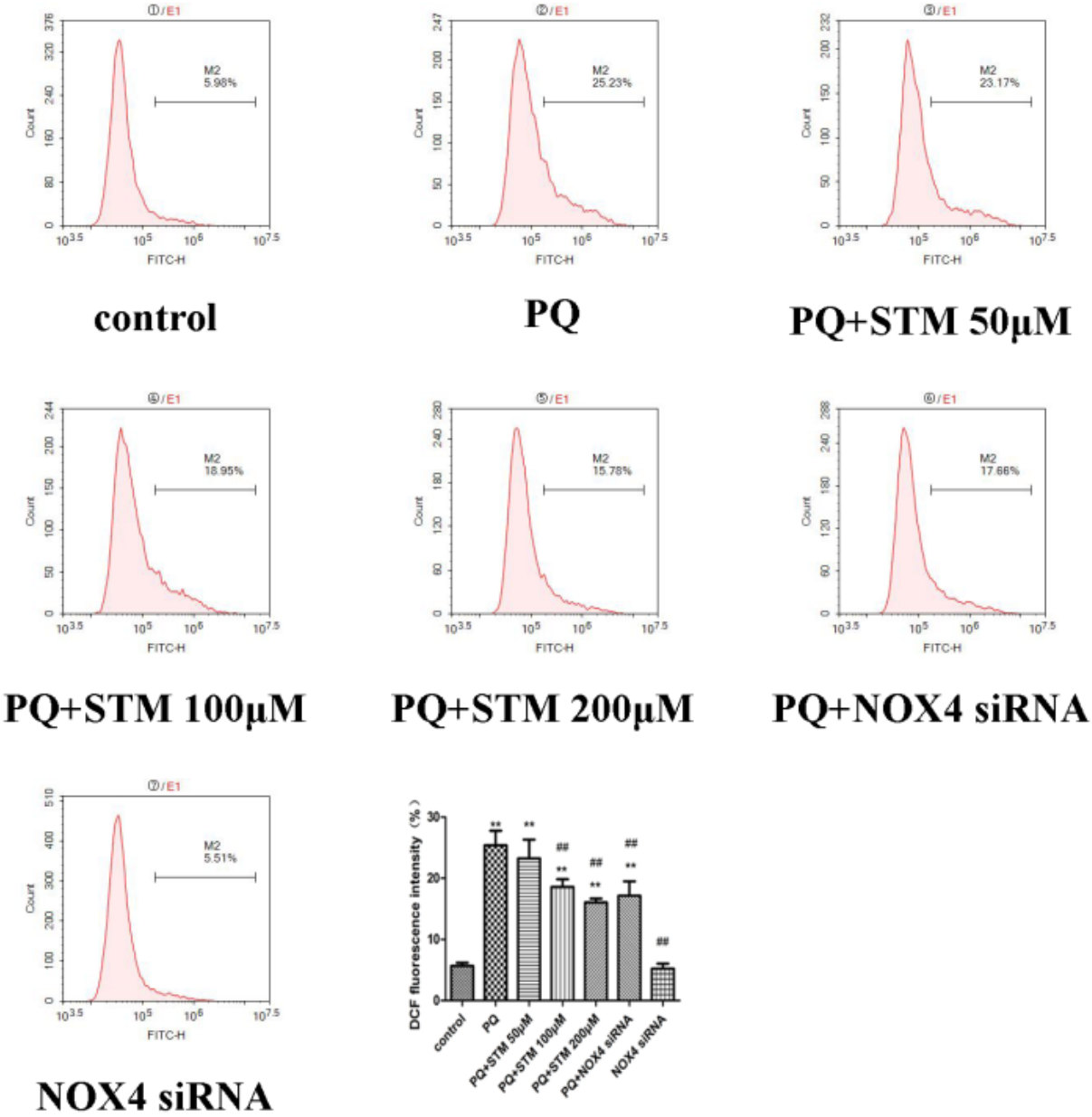

FIGURE 5 - Amelioration of the PQ-induced redox imbalance by STM. PQ exposure significantly increased intracellular DCFH oxidation in A549 cells, as indicated by the DCF fluorescence intensity, suggesting activated iron signaling or peroxynitrite formation. Pretreatment with STM (100 and 200 μM) or NOX4 silencing reduced DCFH oxidation, thus ameliorating the PQ-induced redox imbalance in A549 cells. The data were obtained from at least three independent experiments. The results are represented as the means ± S.D.s. $^{**}p<0.01$ versus control; $^{\#\#}p<0.01$ versus PQ, determined using one-way ANOVA with Tukey's post hoc analysis.

STM impacted the TLR4-NOX4 pathway

As shown in Figure 6, the expression of NOX4 was inhibited by STM or NOX4 siRNA, and TLR4 was suppressed by STM. In addition, NOX4 siRNA did not notably influence TLR4 levels. Overall, STM ameliorated the PQ-induced redox imbalance through the TLR4-NOX4 pathway.

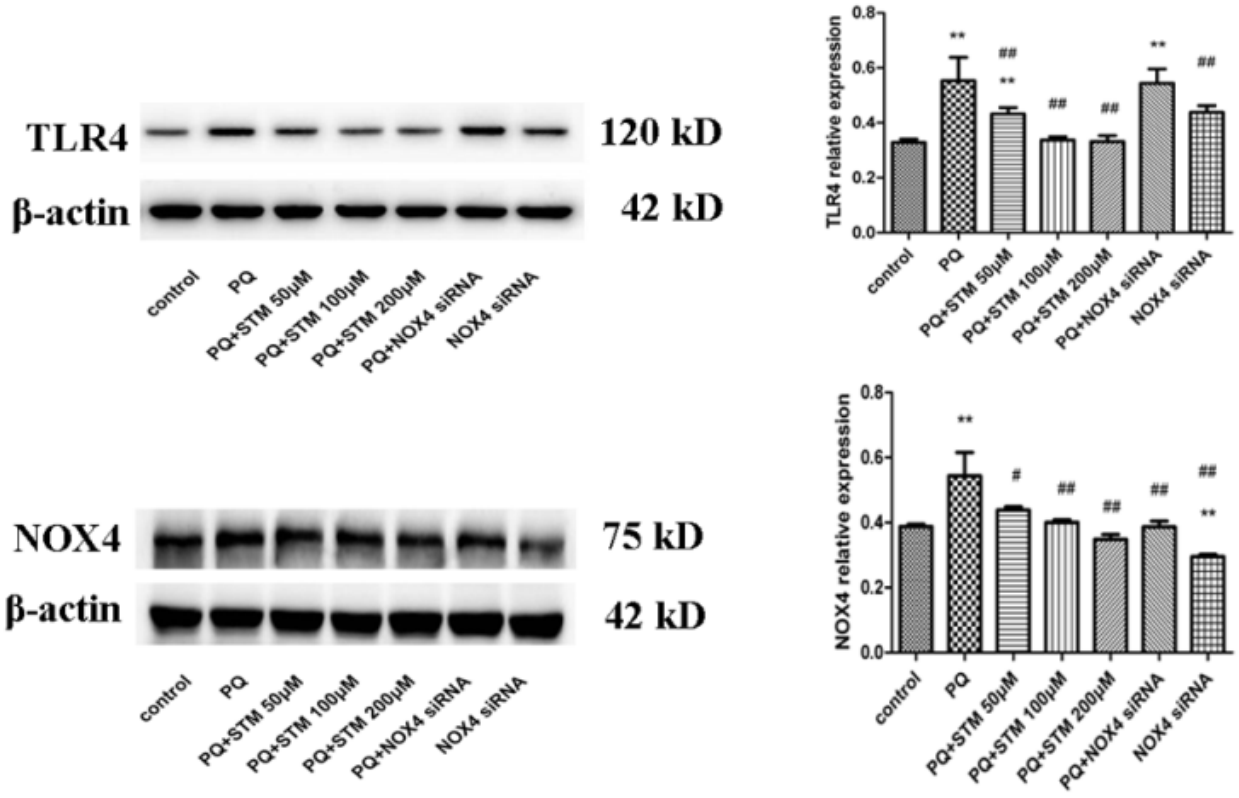

FIGURE 6 - STM inhibited the TLR4-NOX4 pathway in PQ-induced A549 cells. The expression of TLR4 and NOX4 in the PQ group was notably increased compared with that in the control group ($p < 0.01$). In comparison, pretreatment with STM (50, 100 and 200 μM) significantly inhibited TLR4 and NOX4 expression compared with that in the PQ group ($p < 0.01$). NOX4 silencing failed to influence TLR4 expression compared with that in the PQ group ($p < 0.01$). The data were obtained from at least three independent experiments. The results are represented as the means ± S.D.s. $^{**}p<0.01$ versus control; $^{\#}p<0.05$ versus PQ, $^{\#\#}p<0.01$ versus PQ, determined using one-way ANOVA with Tukey's post hoc analysis.

In this study, we evaluated the effect of STM on PQ-induced injury in human lung alveolar epithelial-like cells (A549) to gain evidence for the treatment of PQ-induced lung fibrosis. We found that pretreatment with STM effectively attenuated PQ-induced injury in A549 cells. Additionally, STM improved MMP in PQ-induced A549 cells. The increases in the apoptosis rate, DCFH oxidation, collagen and TLR4-NOX4 signaling induced by PQ were significantly inhibited by STM. Taken together, our results suggested that STM could ameliorate PQ-induced A549 cell injury. In addition, the downregulation of NOX4 by siRNA exerted similar protective effects as STM. Thus, STM attenuated PQ-induced pulmonary epithelial-like cell apoptosis via NOX4-mediated regulation of redox and mitochondrial function.

Great strides have been made in understanding the pathophysiology of PQ-induced pulmonary fibrosis and its treatment. It has been revealed that PQ-induced

redox reactions produce large amounts of reactive oxygen species (ROS) and reactive nitrogen species (RNS) that cause apoptosis and lung epithelial injury (He *et al*., 2016). ROS oxidize unsaturated fatty acids on various biofilms to trigger endoplasmic reticulum stress (ERS) and apoptosis, which exacerbate lung injury and fibrogenesis. PQ exposure can induce apoptosis through the mitochondrial apoptotic pathway in A549 cells, which is mediated by ROS (Cui *et al*., 2019). ROS trigger apoptosis by interacting with mitochondrial permeability transition complex proteins. In response to ROS, the mitochondrial membrane undergoes hyperpolarization, collapsing the MMP and promoting cytochrome C release and subsequent caspase-3 and poly (ADP) polymerase cleavage. Improvements in mitochondrial function can ameliorate the apoptotic effects of PQ on A549 cells (Sun *et al*., 2018). ROS is a generic term for a large family of oxidants derived from molecular oxygen. During oxidative eustress, oxidants are present at low levels, whereas during oxidative distress, an increased oxidant concentration drives aberrant or disrupted redox signaling. The primary oxidants H_2O_2 and superoxide ($O_2^{\cdot-}$), which have extensively documented functions, are major redox signaling agents. Secondary oxidants and electrophiles include 4-hydroxynonenal (HNE) generated by lipid peroxidation and peroxynitrite ($ONOO^-$) formed from $O_2^{\cdot-}$ and nitric oxide (·NO) (Sies *et al*., 2022). DCFH-DA is the most widely used probe for detecting intracellular H_2O_2 and oxidative stress. However, the intracellular redox chemistry of DCFH is complex, and there are several limitations associated with use of the DCF assay for intracellular H_2O_2 measurement. DCFH does not directly react with H_2O_2 to form the fluorescent product DCF. Therefore, DCF fluorescence cannot be used as a direct measure of H_2O_2 levels. DCFH-DA may be used as a redox indicator probe that responds to changes in intracellular iron signaling or peroxynitrite formation (Kalyanaraman *et al*., 2012). Our data revealed that STM significantly reduced DCFH oxidation and increased the MMP, thus inhibiting apoptosis in PQ-treated A549 cells. The present study showed oxidative stress in PQ-treated A549 cells, including a significant increase in the level of MDA, which is the main product of lipid peroxidation. The administration of STM significantly decreased ROS and lipid peroxidation. NADPH oxidases (NOXs) are a family of flavoenzymes that are solely responsible for primary ROS production. Seven isoforms of NOXs exist, and most of them are expressed in fibroblasts and contribute to the pathogenesis of lung fibrosis. Among them, NOX4 is upregulated in idiopathic pulmonary fibrosis, bleomycin-induced lung injury, and lung cancer (Li *et al*., 2021). These results indicate that a reduction in ROS formation and oxidative stress might be one mechanism by which STM improves PQ-induced injury.

Since the pulmonary alveolar epithelium is continuously exposed to considerable amounts of microorganisms in the environment, TLRs expressed in the pulmonary alveolar epithelium are believed to play a critical role in maintaining the homeostasis of the epithelial barrier, which can be disrupted by pathogenic microbes or toxic chemicals such as PQ (Shen *et al*., 2017). It was reported that TLR4 might be a mediator and play an important role in acute lung injury in mice induced by PQ poisoning (Liu *et al*., 2014). Downregulating TLR4 could relieve PQ-induced cytotoxicity in alveolar macrophages (Alizadeh-Tabrizi *et al*., 2017). A similar finding was also obtained in this study: PQ exposure led to the upregulation of TLR4 in human lung alveolar epithelial-like cells (A549). The present study showed that TLR4 expression significantly increased following PQ exposure, and similar trends were observed in downstream molecules of TLR4 (such as TNF-α and IL-8). Additionally, activation of TLR4 signaling triggers the release of oxidation intermediates, including ROS, RNS and cytokines (Ryan *et al*., 2004). The main form of ROS is superoxide anion ($O_2^{\cdot-}$), which is mostly produced by NADPH oxidase (NOX) (Tarafdar, Pula, 2018). Thus, there seemed to be a close interaction between NOX4 and TLR4, which would lead to ROS generation. And Park *et al*. (2004) demonstrated a direct interaction between TLR4 and NOX4 using a yeast two-hybrid pull-down assay and correlated this complex with LPS-induced ROS production. During myeloid differentiation protein 2-induced retinal ischemia reperfusion, NOX4 binds to TLR4, activating the production of tissue-damaging ROS and cytokines, indicating a signal that is downstream of TLR4 (Chen *et al*., 2018). Our data indicated that STM could notably inhibit PQ-induced TLR4-NOX4 signaling activation, thus reducing subsequent oxidant production.

It is well known that oxidative stress due to PQ exposure is considered the foundational mechanism by which pulmonary damage is induced during PQ-induced pulmonary fibrosis. The main sources of PQ-induced ROS production are PQ metabolism in microsomal enzyme systems and mitochondria and the activation of NOX4 in inflammatory and lung target cells (Pourgholamhossein *et al*., 2018). Recently, targeting NOX4 seemed to be a promising strategy to alleviate experimental lung fibrosis (Sato *et al*., 2016; Du *et al*., 2021; Liu *et al*., 2021). Our results indicated that reducing oxidant formation and oxidative stress might be mechanisms by which the antiapoptotic effect of STM is mediated. We also found that STM inhibited PQ-induced NOX4 expression in A549 cells, and the same effect was observed by silencing NOX4 with siRNA, indicating that NOX4 plays a key role in the antiapoptotic effect of STM. Our results indicated that STM modulated redox status and maintained mitochondrial function, probably by inhibiting NOX4 expression, thereby exerting antiapoptotic activity.

CONCLUSION

In conclusion, we demonstrated that pretreatment with STM alleviated PQ-induced A549 cell injury and apoptosis. The protective effect of STM may involve the inhibition of NOX4-stimulated oxidative stress and the downregulation of profibrotic cytokine and inflammatory cytokine production. However, further study is needed to investigate the other pathways involved in the protective effect of STM.

ACKNOWLEDGEMENTS

This work was supported by grants from the Science Foundations of Wuhan City College (2019CYZDKY002), the Science Foundations of Wuhan Municipal Health Commission (WX19Q37) and the Science Foundations of Health Commission of Hubei Province (WJ2019H384).

CONFLICTS OF INTEREST

The authors report no conflicts of interest.

REFERENCES

Alizadeh-Tabrizi N, Malekinejad H, Varasteh S, Cheraghi H. Atorvastatin protected from paraquat-induced cytotoxicity in alveolar macrophages via down-regulation of TLR-4. Environ Toxicol Pharmacol. 2017;49:8-13.

Blanco-Ayala T, Andérica-Romero AC, Pedraza-Chaverri J. New insights into antioxidant strategies against paraquat toxicity. Free Radic Res. 2014;48(6):623-640.

Chen H, Song Z, Ying S, Yang X, Wu W, Tan Q, et al. Myeloid differentiation protein 2 induced retinal ischemia reperfusion injury via upregulation of ROS through a TLR4-NOX4 pathway. Toxicol Lett. 2018;282:109-120.

Chen J, Liu J, Lei Y, Liu M. The anti-inflammation, anti-oxidative and anti-fibrosis properties of swertiamarin in cigarette smoke exposure-induced prostate dysfunction in rats. Aging (Albany NY). 2019;11(22):10409-10421.

Cui S, Nian Q, Chen G, Wang X, Zhang J, Qiu J, et al. Ghrelin ameliorates A549 cell apoptosis caused by paraquat via p38-MAPK regulated mitochondrial apoptotic pathway. Toxicology. 2019;426:152267.

Du JJ, Sun JC, Li N, Li XQ, Sun WY, Wei W. β-Arrestin2 deficiency attenuates oxidative stress in mouse hepatic fibrosis through modulation of NOX4. Acta Pharmacol Sin. 2021;42(7):1090-1100.

Gao F, Zhang Y, Yang Z, Wang M, Zhou Z, Zhang W, et al. Arctigenin Suppressed Epithelial-Mesenchymal Transition Through Wnt3a/β-Catenin Pathway in PQ-Induced Pulmonary Fibrosis. Front Pharmacol. 2020;11:584098.

Gawarammana IB, Buckley NA. Medical management of paraquat ingestion. Br J Clin Pharmacol. 2011;72(5):745-757.

He Y, Zou L, Zhou Y, Hu H, Yao R, Jiang Y, et al. Adiponectin ameliorates the apoptotic effects of paraquat on alveolar type II cells via improvements in mitochondrial function. Mol Med Rep. 2016;14(1):746-752.

Kalyanaraman B, Darley-Usmar V, Davies KJ, Dennery PA, Forman HJ, Grisham MB, et al. Measuring reactive oxygen and nitrogen species with fluorescent probes: challenges and limitations. Free Radic Biol Med. 2012;52(1):1-6.

Li S, Wang Q, Tao Y, Liu C. Swertiamarin Attenuates Experimental Rat Hepatic Fibrosis by Suppressing Angiotensin II-Angiotensin Type 1 Receptor-Extracellular Signal-Regulated Kinase Signaling. J Pharmacol Exp Ther. 2016;359(2):247-255.

Liu Q, Zheng B, Zhang Y, Huang W, Hong Q, Meng Y. Alamandine via MrgD receptor attenuates pulmonary fibrosis via NOX4 and autophagy pathway. Can J Physiol Pharmacol. 2021;99(9):885-893.

Liu K, Zhan Z, Gao W, Feng J, Xie X. Cyclosporine attenuates Paraquat-induced mitophagy and pulmonary fibrosis. Immunopharmacol Immunotoxicol. 2020;42(2):138-146.

Liu W, Shan LP, Dong XS, Liu Z. Toll-like receptor 4 implicated in acute lung injury induced by paraquat poisoning in mice. Int J Clin Exp Med. 2014;7(10):3392-3397.

Li ZM, Xu SY, Feng YZ, Cheng YR, Xiong JB, Zhou Y, et al. The role of NOX4 in pulmonary diseases. J Cell Physiol. 2021;236(3):1628-1637.

Loveman E, Copley VR, Colquitt JL, Scott DA, Clegg AJ, Jones J, et al. The effectiveness and cost-effectiveness of treatments for idiopathic pulmonary fibrosis: systematic review, network meta-analysis and health economic evaluation. BMC Pharmacol Toxicol. 2014;15:63.

Novaes RD, Gonçalves RV, Cupertino MC, Santos EC, Bigonha SM, Fernandes GJ, et al. Acute paraquat exposure determines dose-dependent oxidative injury of multiple organs and metabolic dysfunction in rats: impact on exercise tolerance. Int J Exp Pathol. 2016;97(2):114-124.

Park HS, Jung HY, Park EY, Kim J, Lee WJ, Bae YS. Cutting edge: direct interaction of TLR4 with NAD(P)H oxidase 4 isozyme is essential for lipopolysaccharide-induced production of reactive oxygen species and activation of NF-kappa B. J Immunol. 2004;173(6):3589-3593.

Pourgholamhossein F, Rasooli R, Pournamdari M, Pourgholi L, Samareh-Fekri M, Ghazi-Khansari M, et al. Pirfenidone protects against paraquat-induced lung injury and fibrosis in mice by modulation of inflammation, oxidative stress, and gene expression. Food Chem Toxicol. 2018;112:39-46.

Ryan KA, Smith MF Jr, Sanders MK, Ernst PB. Reactive oxygen and nitrogen species differentially regulate Toll-like receptor 4-mediated activation of NF-kappa B and interleukin-8 expression. Infect Immun. 2004;72(4):2123-2130.

Saravanan S, Pandikumar P, Prakash Babu N, Hairul Islam VI, Thirugnanasambantham K, Gabriel Paulraj M, et al. In vivo and in vitro immunomodulatory potential of swertiamarin isolated from Enicostema axillare (Lam.) A. Raynal that acts as an anti-inflammatory agent. Inflammation. 2014;37(5):1374-1388.

Sato N, Takasaka N, Yoshida M, Tsubouchi K, Minagawa S, Araya J, et al. Metformin attenuates lung fibrosis development via NOX4 suppression. Respir Res. 2016;17(1):107.

Shen H, Wu N, Liu Z, Zhao H, Zhao M. Epigallocatechin-3-gallate alleviates paraquat-induced acute lung injury and inhibits upregulation of toll-like receptors. Life Sci. 2017;170:25-32.

Sies H, Belousov VV, Chandel NS, Davies MJ, Jones DP, Mann GE, et al. Defining roles of specific reactive oxygen species (ROS) in cell biology and physiology. Nat Rev Mol Cell Biol. 2022;23(7):499-515.

Sun DZ, Song CQ, Xu YM, Wang R, Liu W, Liu Z, et al. Involvement of PINK1/Parkin-mediated mitophagy in paraquat- induced apoptosis in human lung epithelial-like A549 cells. Toxicol In Vitro. 2018;53:148-159.

Tarafdar A, Pula G. The Role of NADPH Oxidases and Oxidative Stress in Neurodegenerative Disorders. Int J Mol Sci. 2018;19(12):3824.

Wu T, Li J, Li Y, Song H. Antioxidant and Hepatoprotective Effect of Swertiamarin on Carbon Tetrachloride-Induced Hepatotoxicity via the Nrf2/HO-1 Pathway. Cell Physiol Biochem. 2017;41(6):2242-2254.

Wu T, Zhang Q, Song H. Swertiamarin attenuates carbon tetrachloride (CCl4)-induced liver injury and inflammation in rats by regulating the TLR4 signaling pathway. Braz J Pharm Sci. 2018;54(4):e17449.

Wynn TA. Common and unique mechanisms regulate fibrosis in various fibroproliferative diseases. J Clin Invest. 2007;117(3):524-529.

Zhang Q, Chen K, Wu T, Song H. Swertiamarin ameliorates carbon tetrachloride-induced hepatic apoptosis via blocking the PI3K/Akt pathway in rats. Korean J Physiol Pharmacol. 2019;23(1):21-28.

Received for publication on 05th July 2022
Accepted for publication on 04th May 2023